European Journal of Radiology 110 (2019) 121–127

Contents lists available at ScienceDirect

European Journal of Radiology

journal homepage: www.elsevier.com/locate/ejrad

Research article

Automatic rib cage unfolding with CT cylindrical projection reformat in polytraumatized patients for rib fracture detection and characterization: Feasibility and clinical application

Ayla Urbaneja[a,*], Jacques De Verbizier[a], Anne-Sophie Formery[a], Catalina Tobon-Gomez[b], Lionel Nace[c], Alain Blum[a], Pedro Augusto Gondim Teixeira[a]

[a] Service d'Imagerie Guilloz, Hôpital Central, Centre Hospitalier Universitaire de Nancy, 29 Ave du Maréchal de Lattre de Tassigny, Nancy, 54035, France
[b] Canon Medical Visualization Systems, Edinburgh, UK
[c] Emergency and Reanimation Department, Hôpital Central, Centre Hospitalier Universitaire de Nancy, 29 Ave du Maréchal de Lattre de Tassigny, Nancy, 54035, France

ARTICLE INFO

Keywords:
Rib cage
Image processing
Rib fractures
Multiple trauma
Computed tomography

ABSTRACT

Objectives: To assess the use of CT with unfolded cylindrical projection (UCP) for rib fracture detection and characterization.

Methods: The images from 60 polytraumatized patients who underwent whole body CT were evaluated for the presence and characterization of rib fractures (displaced or not, single or multiple). Two readers independently evaluated conventional CT images and UCP images in two readout sessions at least one month apart. All readouts were timed. A gold standard was established by two radiologists with 12 and 22 years of clinical experience based on the combined analysis of conventional and UCP reformats.

Results: Using UCP, the mean evaluation time was 27%–54% shorter ($P = 0.01$ and < 0.0001) while maintaining a comparable diagnostic performance (sensitivity and specificity of 68.4–79.1% and 99.5–99.6% for conventional reformats and 70.6–91.0% and 96.8–97.7% for UCP) and a good reproducibility (Kappa of 0.71). The multiple fracture detection ratio of UCP was similar to that of conventional reformats (> 80%). There were more false positives and false negatives using UCP and displaced fractures were harder to characterize.

Conclusion: UCP yielded a diagnostic performance similar to that of conventional reformats for the detection of rib fractures with a good reproducibility and a noticeable reduction in evaluation time.

1. Introduction

Rib cage evaluation to detect costal fractures is a tedious but essential task for polytraumatized patients. Rib fractures, in addition to pain and discomfort, may be associated with clinically important complications such as hypoventilation (flail thorax syndrome), pneumonia, lung contusion pneumothorax, hemothorax and death [1–3]. CT is the imaging method of choice for the evaluation of polytraumatized patients allowing a thorough and accurate assessment of musculoskeletal, thoracic and abdominal injuries [4,5]. Rib fractures can be of various types (unicortical, bi cortical, hair-like, trabecular only) some of which are difficult to diagnose on CT. Ribs are long arched bones with a posterior cylindrical shape and a flatter anterior shape. Ribs have a downward obliquity which is variable depending on various factors (e.g. rib level, patient sex, size, age etc.) [6]. This anatomy makes rib cage CT evaluation a meticulous and time consuming process because no orthogonal plane is optimal for visualization of all the ribs of an individual. Moreover, rib fractures are usually of secondary importance compared to visceral/vascular lesions, and prompt image analysis is required for CT exams of polytraumatized patients. These factors explain, at least partially, the large number of false negatives for the diagnosis of rib fractures.

Various studies have demonstrated the improvement in rib cage evaluation time by curved planar reformats in the long axis of each pair of right and left ribs, which allows all ribs to be depicted in the same plane, facilitating analysis [7,8]. Recently, this type of reformat has been shown to improve the sensitivity of rib fracture detection among less experienced readers (interns and residents) [7,9]. Until recently a single technique allowing this type of image reformat was proposed by a sole vendor limiting the availability of unfolded rib cage reformats. In

* Corresponding author at: Service d'Imagerie Guilloz, Hôpital Central, Centre Hospitalier Universitaire de Nancy 29, Avenue du Maréchal de Lattre de Tassigny, 54035, Nancy Cedex, France.
E-mail address: ayla.urbaneja7@etu.univ-lorraine.fr (A. Urbaneja).

https://doi.org/10.1016/j.ejrad.2018.11.011
Received 10 October 2018; Received in revised form 10 November 2018; Accepted 12 November 2018

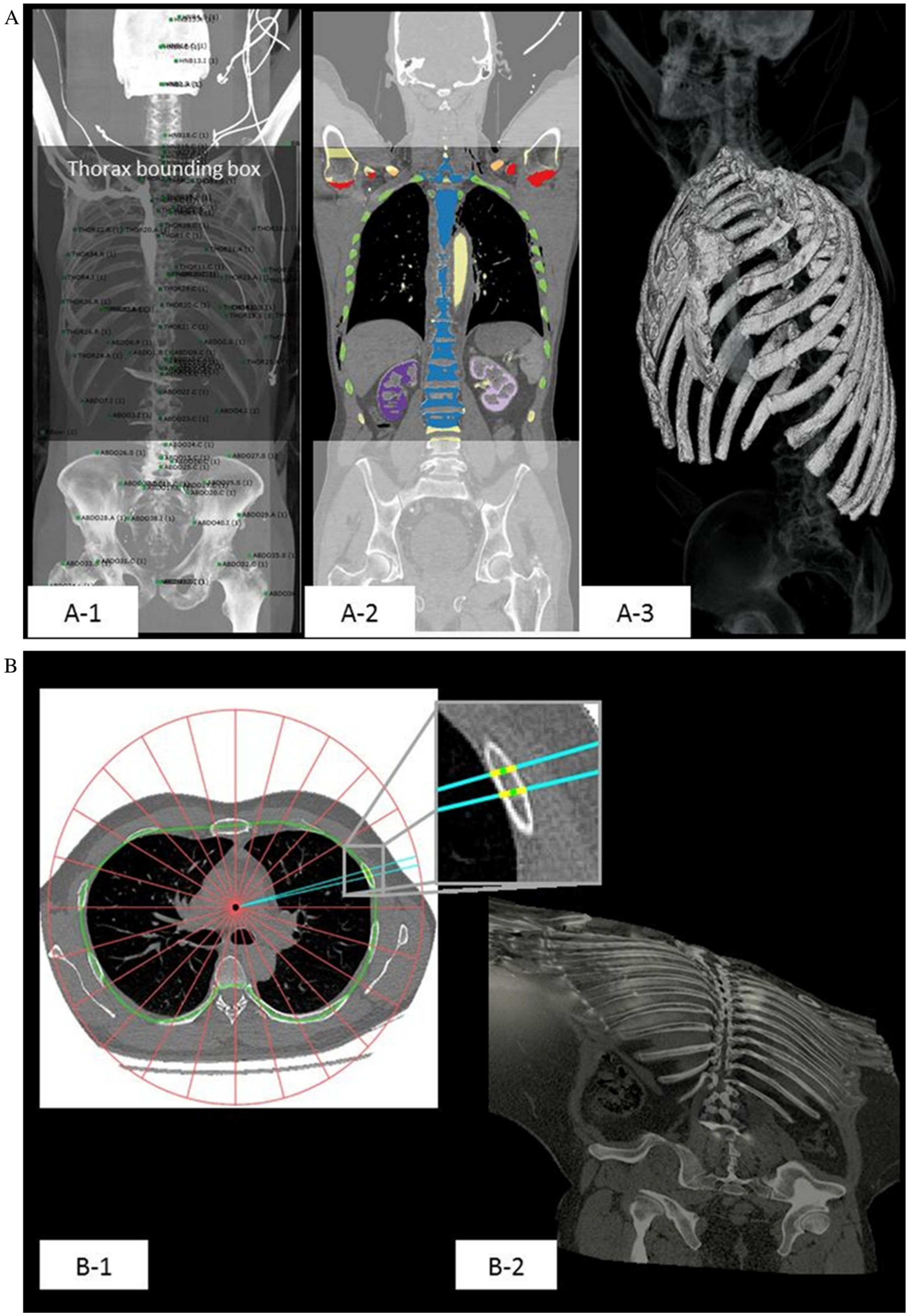

Fig. 1. Schematic overview of the unfolded cylindrical projection algorithm. The algorithm has two steps: rib cage segmentation and unfolding. Automatically detected anatomical landmarks are used to compute a bounding box (A-1) and threshold the bony thoracic wall. This wall is registered to an atlas to transfer previously defined labels (A-2). The rib cage segmentation is polished and input to the unfolding step (A-3). The unfolding step computes a 3D manifold that intersects the rib cage segmentation (B-1). A cylindrical projection maps the points from the 3D manifold to the 2D image (B-2).

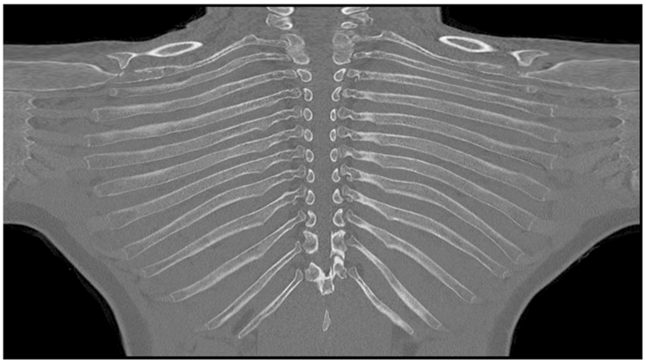

Fig. 2. Rib cage post-processing by rib UCP with a bone window of a 28 year-old polytraumatized male patient. In this image all 24 ribs are displayed entirely in a frontal plane. In the central part of the image, the dorsal column is displayed and at the lateral edges of the image the lateral extremities of the sternum are displayed. Note that a part of the anatomic vertebral contours is maintained and the increased distortion in the first and second ribs. There were no fractures ribs in this patient.

this work, we sought to evaluate an alternative method of automatic unfolding of the rib cage which is completely distinct from curved planar reformats. This technique automatically creates a 2D cylindrical projection of the whole rib cage based on a complex 3D manifold system following the long axis of the ribs (herein named unfolded cylindrical projection - UCP) [10]. The diagnostic performance and evaluation time of this algorithm for the detection of rib fractures in polytraumatized patients is compared to that of conventional multiplanar reformats. We hypothesize that UCP reformats could be a viable alternative to optimize rib cage evaluation in a trauma setting.

2. Materials and methods

2.1. Population

Images from 60 consecutive patients who underwent whole body CT from November 2016 to January 2017 were retrospectively analyzed. All subjects were over 18 years-old and were imaged in a context of severe polytrauma. All studies performed comprised a whole body pre-contrast acquisition and post-contrast acquisition (arterial whole body acquisition and portal phase abdominal acquisition). Pre-contrast images were anonymized. Three patients were excluded due to the absence of a pre-contrast acquisition. In our institution, ethics committee approval is not necessary for retrospective studies using completely anonymized patient data and no changes in the acquisition protocol.

2.2. Acquisition technique and reconstruction procedure

All images were acquired with 320 detector-row CT scanner (Aquilion ONE, Canon Medical Systems, Otawara, Japan) using a helical acquisition mode and the following parameters: 135 kV, 100–500 mA s (depending on automatic exposure modulation), 36 cm FOV, 512 × 512 matrix, 0.5 mm slice thickness, 0.5 s gantry rotation speed, 0.8 pitch. Images were reconstructed using iterative reconstruction (AIDR 3D, Canon Medical Systems, Otawara, Japan) and bone kernels.

Original DICOM images were transferred to an independent workstation (Vitrea version 7.5 Vital Images, Minnetonka, USA). The UCP algorithm includes two automatic steps: segmentation and unfolding (Fig. 1) [10]. For segmentation, key anatomical landmarks are automatically detected and used to compute a bounding box of interest. Areas outside the box of interest are discarded (e.g. head, pelvis, legs). The HU values at landmark locations are sampled for each case to threshold the bony thoracic wall. This bony thoracic wall is registered to an atlas to transfer previously defined labels (rib cage, vertebrae and sternum). The rib cage segmentation is polished by tracing missing sections within each rib. For unfolding, a 3D manifold that intersects the rib cage segmentation is created. A cylindrical projection maps the points from the 3D manifold to the 2D image (Fig. 1). As a result an image series depicting all ribs in a complex coronal plane is created (Fig. 2).

2.3. Data analysis

Data analysis was performed on the same workstation used for UCP post-processing. All readers were blinded to clinical information. Images were evaluated using a fixed window level (L = 350HU, W = 2700HU). Ribs were evaluated one-by-one for the presence or absence of recent fractures. A rib was considered fractured from the moment when there was a clear break in cortical continuity or when there was a focal change in cortical bone contour. Fractured ribs were further classified as displaced or not (fractures with more than 1.5 mm displacement was considered as displaced) and single or multiple.

Two radiologists with six years and 12 years of clinical experience (JD and PGT) (readers 1 and 2) evaluated independently UCP images (conventional reformats not available) and conventional reformats (the analysis was based mainly on axial images but coronal and sagittal reformats were available to the readers) in two readout sessions performed at least one month apart. Evaluation was timed and triangulation was not available.

Reader 2 also subjectively evaluated the quality of UCP using the grading system below. Quality assessment was not included in the rib fracture evaluation time. Reformat related artifacts were characterized by distortion of rib contours in the complex coronal plane.

1 = One or more ribs completely obscured by artifacts
2 = Marked artifacts with no confidence for analysis
3 = Low confidence in the analysis of rib structure
4 = Presence of artifacts with good confidence in the analysis of rib structure
5 = High confidence in analysis of rib structure, perfect image

After the initial readouts a gold standard was established in consensus by two radiologists: reader 3 with 22 years of clinical experience in musculoskeletal CT imaging and reader 2. Evaluation time was not considered and all available image series were available for analysis (original axials, multiplanar reformats, UCP). Triangulation was possible between all the reformats available including UCP.

False positive and false negative cases were reviewed and analyzed for the presence of motion artifacts, UCP related artifacts, old fractures; physiologic rib contour changes, hair-like and trabecular fractures (focal change in rib contour with no cortical continuity loss). The presence of fractures located close to the costo-chondral and costo-vertebral joints was also considered.

2.4. Statistics

The diagnostic performance of conventional reformats and UCP analysis for the identification of fractured ribs was assessed using the created gold standard as reference. The frequency of correct diagnosis of displaced fractures and multiple fractures was calculated. Interobserver reproducibility for the identification of fractured ribs was evaluated by the calculation of the kappa index. Kappa values of 0-0.20 were considered to represent slight; 0.21-0.4, fair; 0.41-0.60, moderate; 0.61-0.80, good; 0.81–1, excellent agreement. A paired student's *t*-test was used to evaluate the time differences between conventional reformat analysis and UCP analysis. A *P* value of 0.05 was considered as the threshold of statistical significance. Time measurements are presented as minutes (m) seconds (s).

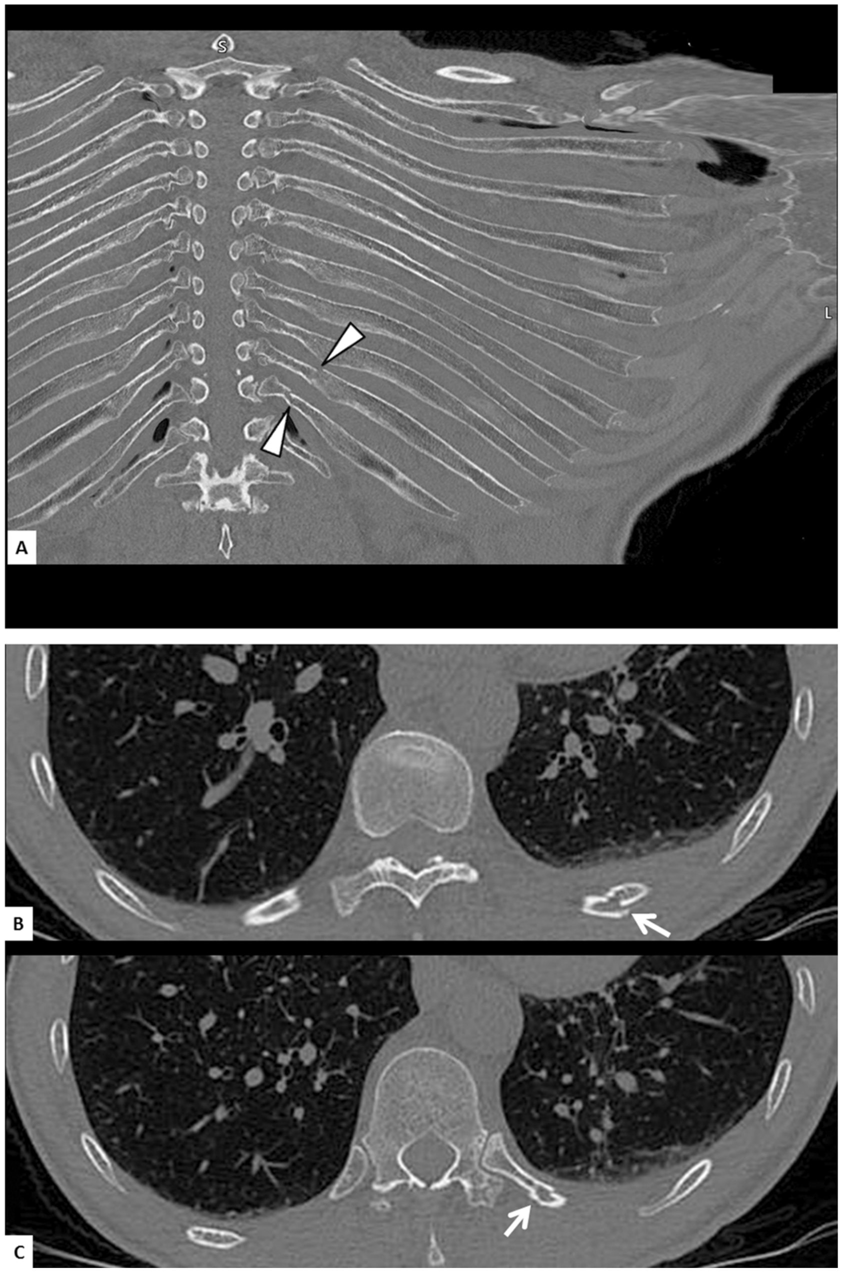

Fig. 3. A) Rib cage UCP with a bone window level of a 54 year-old polytraumatized woman. There is a single non-displaced fracture of the 10th and the 11th left ribs (arrow heads). Axial CT images of the same patient (B and C) demonstrating the corresponding fractures of the 10th and 11th respectively (thin arrows).

3. Results

Among the 57 subjects included there were 38 males and 19 females (M/F ratio = 2) aged from 18 to 86 years old (mean 42.1 ± 19.3). Thirty-three of these patients were diagnosed with single or multiple rib fractures. A total of 1368 ribs were analyzed, 177 ribs were considered to be fractured in the gold standard analysis. Twenty-nine rib fractures were considered to be displaced and 48 ribs presented multiple fractures (Fig. 3).

Rib UCP image reconstruction was successful in all patients. The interobserver variability was considered to be good for conventional and UCP reformats with Kappa values of 0.77 and 0.71 respectively. The mean UCP image quality was 4.3 ± 1 on a five point scale. Artifacts were mainly related to morphologic distortion of the first and second ribs. In one patient the proximity with the inferior angle of the scapula generated contour abnormalities in the adjacent rib, and in another patient pleural calcifications generated similar findings (Fig. 4). Image quality was graded below three in 10 patients (17.5%), although in these cases only a small number of ribs (maximum of three ribs) were affected by reconstruction artifacts.

Rib analysis with conventional reformats yielded sensitivity, specificity, PPV and NPV of 68.4–79.1%, 99.5–99.6%, 95.3–96.6% and 95.5–97% for both readers (Table 1). With UCP these figures were similar with a 70.6–91%, 96.8–98.2%, 80.1–85% and 95.7–98.6% of sensitivity, specificity, PPV and NPV for both readers. With conventional reformats, the mean evaluation time varied from 0 m 40 s to 5 m 30 s for reader 1 and from 3 m 56 s to 12 m 3 s for reader 2 (mean = 1 m 39 s ± 1 m 6 s and 6 m 9 s ± 1 m 34 s respectively). The mean evaluation time with UCP was significantly shorter for both readers (1 m 12 s ± 43 s and 2 m 48 s ± 60 s for readers 1 and 2 respectively) (P = 0.01 and $P <$ 0.001 for readers 1 and 2). This represents a 27.3% to 54.5% mean reduction in the evaluation time.

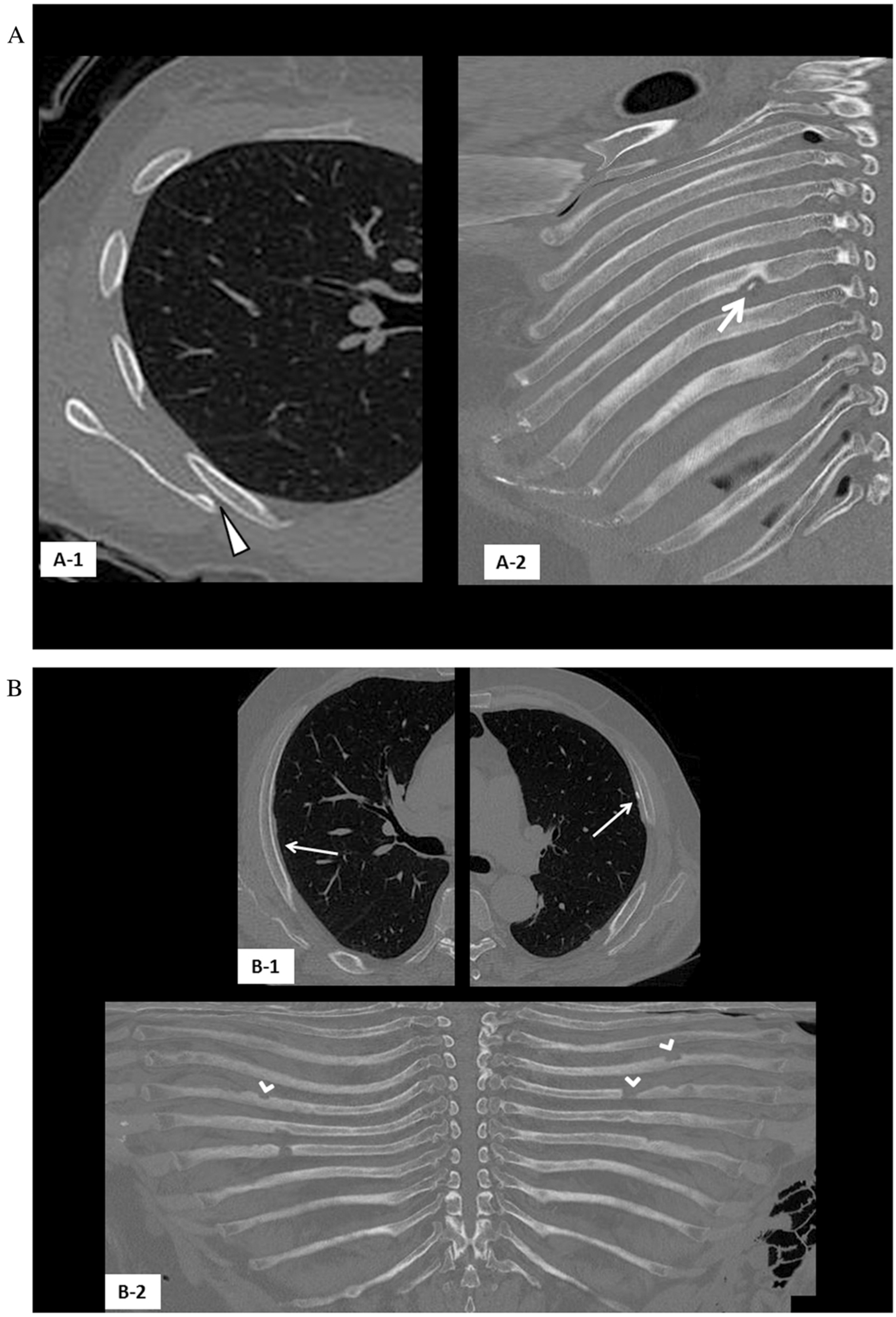

Fig. 4. Examples algorithm related artifacts with UCP. Rib cage UCP with a bone window level of a 36 year old woman (A) and of a 69 year old woman (B). In (A) the close proximity between the with the inferior angle of the scapula generated contour abnormalities in the 6th right rib on the axial image (A-1) (arrowhead) and the corresponding UCP image (A-2) (arrow). In the second case (B), pleural calcifications (arrows in B-1) generated contour abnormalities with the adjacent ribs on UCP images (B-2) in which artefactual contour abnormalities can be seen in various ribs (arrowheads).

There were 56 and 37 false negatives as well as six and five false positives for readers 1 and 2 respectively using conventional reformats. The imaging features associated with false positive and negative ribs with conventional and UCP reformats are presented in Table 2. Hair like and trabecular fractures represent the biggest portion of false negative cases (43 and 33 respectively for readers 1 and 2). Rib numbering error, fracture location close to costo-chondral or costo-vertebral joints and motion artifacts were associated with 5.4%–8.1 % of false negatives. With UCP images hair-like and trabecular fractures were associated with false negative results in 50% and 53.8% of cases followed by fractures located either near the costo-chondral or costo-vertebral joints in 19.2% and 43.8% of cases. Reconstruction artifacts were associated in less than 5% of false negative rib fracture cases. If the false positive and negative results of both readers were considered, UCP related artifacts were associated with 4.7% of cases. There was a higher number of false positives when UCP visualization was used for both readers (six and five false positives with conventional and 22 and 38 false positive with UCP visualization respectively for the reader one and two).

Table 1
Comparison between the diagnostic performances of the conventional reformat and UCP analysis.

	Conventional Reformat		UCP analysis	
	Reader 1	Reader 2	Reader 1	Reader 2
True positive	121	140	125	161
True negative	1185	1186	1169	1153
False positive	6	5	22	38
False negative	56	37	52	16
Sensitivity	68.4%	79.1%	70.6%	91%
Specificity	99.5%	99.6%	98.2%	96.8%
PPV	95.3%	96.6%	85%	80.1%
NPV	95.5%	97.0%	95.7%	98.6%
Mean evaluation time[a]	1 m 39 s (± 1 m 06 s)	6 m 9 s (± 1 m 34 s)	1 m 12 s (± 43 s)	2 m 48 s (± 1 m 0 s)

PPV: Positive Predictive Value.
NPV: Negative Predictive Value.
[a] Data expressed in minutes (m) and seconds (s).

Table 2
Imaging features associated with false positive and negative analysis with conventional reformat and UCP ribcage reformat.

	Conventional reformat		UCP analysis	
	Reader 1	Reader 2	Reader 1	Reader 2
False positives				
Associated old fractures	2	4	13	14
Physiologic rib irregularities	1	1	4	8
Motion artifacts	0	0	4	3
Numbering error	2	0	0	0
Algorithm artifacts	0	0	1	2
Indeterminate	1	0	0	11
TOTAL	**6**	**5**	**22**	**38**
False negatives				
Hair-like and trabecular fractures	43	33	28	8
Associated old fractures	0	1	1	0
Motion artifacts	0	1	2	0
Fracture location	1	0	9	7
Algorithm artifacts	0	0	3	0
Numbering error	2	2	0	1
Undetermined	10	0	9	0
TOTAL	**56**	**37**	**52**	**16**

Moreover, with UCP, old rib fractures were present in 36.8%–59.1% of the false positive ribs. Physiologic alterations in rib contours were associated with 18.2%–21.1% false positive ribs. Reconstruction artifacts were associated in 4.5%–5.3% of false positive rib fracture cases. Examples of false positive and negative with UCP images are presented in Fig. 5.

Among the rib fractures evaluated, conventional reformats allowed the correct distinction between single and multiple fractures in 81% and 89.3% while with UCP images 80.8%–88.2% of the fractures were correctly classified for both readers. Similarly, using conventional reformats 83.5% and 97.1% of the fractures were correctly categorized as displaced or non-displaced. UCP images demonstrated a lower performance for the distinction between displaced and non-displaced fractures particularly for reader 1 with 69.6%–86.3% of correct descriptions.

4. Discussion

The UCP algorithm allowed rib cage visualization with a considerable reduction in readout time (up to 50%) while maintaining a similar diagnostic performance with respect to conventional images (sensitivity of 68–79% and 70–91% and specificity of 99% and 97–98% for conventional and UCP reformats respectively). Compared to the previously reported approach to rib cage unfolding with curved planar reformats, UCP yielded a similar diagnostic performance and a comparable analysis time reduction [7–9,11,12]. Additionally, rib cage unfolding with curved planar reformats, for some authors, require manual input in the post-processing in up to 30% of cases whereas UCP is fully automatic [8]. The interobserver reproducibility for rib fracture identification using UCP was considered to be good (ICC = 0.71). In clinical practice this performance and reproducibility are likely to be increased by the use of synchronous triangulation, which allows easy confirmation of equivocal fractures in other imaging planes. This feature is available on the workstation used but was disabled to provide a better appreciation of the diagnostic performance and potential weaknesses of UCP images. This data indicates that UCP rib cage reformats represent a valid option to improve the effectiveness of rib fractures detection in polytraumatized patients.

Compared to the conventional reformats, there were more false positive rib fractures when UCP was used for fracture detection (5–6 versus 22–38 respectively). The presence of old rib fractures were at least partially responsible for a significant portion of these interpretation errors (36.8–59.1% of false positive cases). This could be explained by callus related changes in rib contour which may be similar to contour changes seen in trabecular fractures on UCP images. Similarly, physiologic focal changes in rib contour were also found in association with false positive cases. False negative interpretations were mainly related to fracture type (hair-like and trabecular fractures) and to fracture location (adjacent to costo-chondral and costo-vertebral joints) (Figs. 4 and 5). Khung et al. reported similar causes for misinterpretation using rib curved planar reformat rib cage unfolding [11]. UCP image quality was considered good (4.3 in a 5 point grading scale) and although algorithm related distortions hindered interpretation of some ribs in 17% of patients, these artifacts were only related to a small number of misinterpretations (4.7%). A similar frequency of misinterpretations has been reported in the literature using curved planar reformats [12]. These results indicate that, in clinical practice, conventional reformats should be used to confirm equivocal factures seen in unfolded rib images.

UCP provides an anatomical view of the ribs with images that can be browsed through as a conventional image series preserving a part of the rib's anatomic contours and keeping thoracic wall soft tissues in the image. Curved planar reformats on the other hand, depict the rib gage with no surrounding soft tissues evaluating each rib with radial reformats thought the rib central axis. UCP showed a detection ratio for multiple fractures similar to that of conventional reformats (> 80%). Displaced fractures, on the other hand, were harder to characterize on UCP images (69.6–86.3% detection ratio) which is probably related to changes in fracture disposition caused by the rib unfolding process. Although not directly evaluated in this study the presence of peri-costal soft tissue on UCP images may assist fracture detection by allowing the visualization of associated findings such as lung parenchymal contusions, hematoma and costal cartilage fractures. Since the whole thoracic wall is present on UCP images, sternal and vertebral fractures could also be identified. Further studies are necessary to explore these matters and to evaluate UCP for the detection of lytic bone lesions such as rib metastasis or costal multiple myeloma lesions [13,14].

Some limitations of this study need to be acknowledged. There was no confirmation of the rib fractures identified in the gold standard readout and there was no correlation of the fractures with clinical symptoms. However, CT is deemed to have a high performance for fracture detection in long bones. Moreover, the gold standard was established with all reformat planes available, with the use of synchronous triangulation and by highly experienced readers (12 and 22 years of clinical experience in musculoskeletal radiology). A single acquisition protocol was evaluated. Some protocol settings (FOV, acquisition type, pitch etc.) could have influenced the quality of the unfolded rib reformats and hence the diagnostic performance. Due to the retrospective nature of this study and since the examinations were

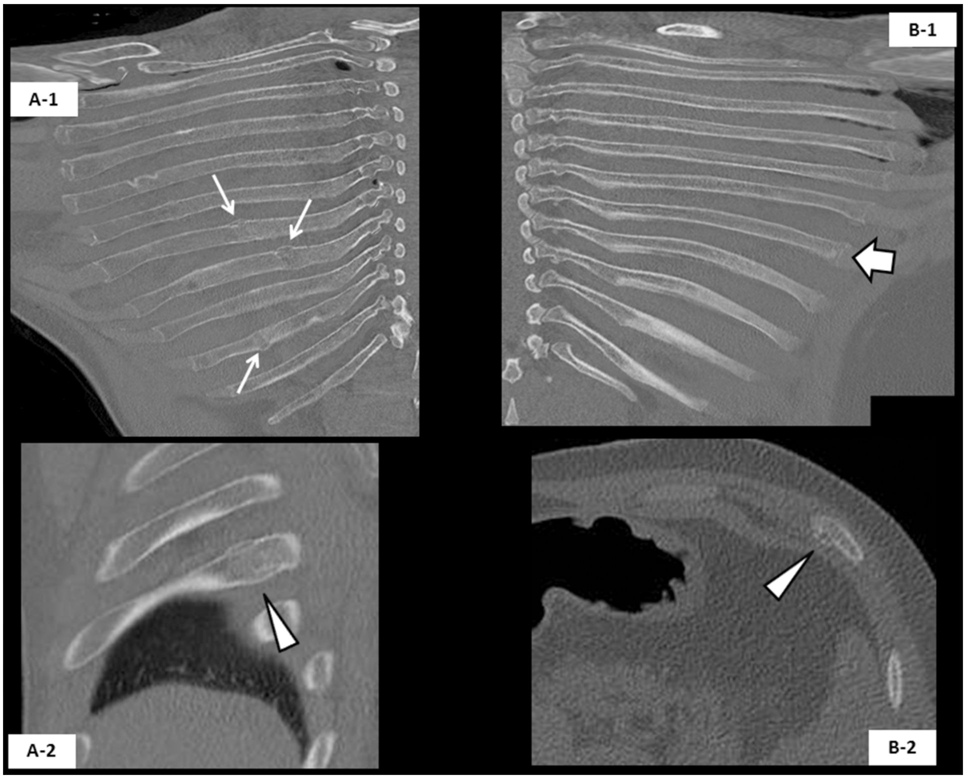

Fig. 5. False positive and negative examples with UCP images. A) UCP image of a 51 year-old man (A) and who presented old rib fractures. Rib contour abnormalities seen in the 7th, 8th and 10th right ribs (arrows in A-1) were difficult to interpret and corresponded to old fractures on conventional sagittal reformats. The old rib fractures in the 7th right rib can be seen in figure A-2 (arrowhead). B) UCP image of a 30 year-old man with a hair-like fracture of the 7th left rib that was not diagnosed by readers on the unfolded rib view (fat arrow in B-1). The fracture was clearly seen as a cortical discontinuity and irregularity on axial images (arrowhead in B-2).

performed in polytraumatized patients in an emergency setting protocol optimization was not possible. The severity of thoracic trauma and the diagnosis of associated findings were not evaluated in this study. Finally, this study was limited to the analysis of rib fractures and further investigation is necessary to ascertain the role of this technique in the evaluation other lesions such as spinal and sternal fractures, and lytic bone lesions of the thoracic wall.

In conclusion, UCP rib cage reformats yielded a diagnostic performance similar to that of conventional reformats for the detection of rib fractures with a good reproducibility and an important reduction in evaluation time. The performance of UCP was also similar to the previously described technique using curved planar rib reformats, underscoring the validity of UCP as an alternative solution, further increasing the availability of unfolded rib cage reformats in clinical practice. Despite the good diagnostic performance, equivocal findings on unfolded rib images should be correlated with conventional reformats to avoid errors related to fracture sequelae, fracture type and in-rib fracture location as well as for the evaluation of fracture displacement.

Conflict of interest

Two authors involved in this work, (P.A. G. T. and A.B.) participate on a non-remunerated research contract with Canon Medical systems, developer of the software used for rib cage unfolding. The author (C. T-G) is an employee of Canon medical systems and worked in the development of the reconstruction algorithm used. This author had no control of patient inclusion, has not performed data analysis or participated in any way that might present a conflict of interest. The other authors have no potential conflicts of interest to disclose.

Funding

The authors state that this work has not received any funding.

References

[1] J.B. Holcomb, N.R. McMullin, R.A. Kozar, M.H. Lygas, F.A. Moore, Morbidity from rib fractures increases after age 45, J. Am. Coll. Surg. 196 (4) (2018) 549–555.

[2] E.M. Bulger, M.A. Arneson, C.N. Mock, G.J. Jurkovich, Rib fractures in the elderly, J. Trauma Acute Care Surg. 48 (6) (2000) (Internet) Available from: http://journals.lww.com/jtrauma/Fulltext/2000/06000/Rib_Fractures_in_the_Elderly.7.aspx.

[3] R. Kent, W. Woods, O. Bostrom, Fatality risk and the presence of rib fractures, Ann. Adv. Automot. Med. Annu. Sci. Conf. 52 (2008) 73–84.

[4] S. Huber-Wagner, R. Lefering, L.-M. Qvick, M. Körner, M.V. Kay, K.-J. Pfeifer, et al., Effect of whole-body CT during trauma resuscitation on survival: a retrospective, multicentre study, Lancet 373 (9673) (2018) 1455–1461.

[5] P. Hilbert, K. zur Nieden, G.O. Hofmann, I. Hoeller, R. Koch, R. Stuttmann, New aspects in the emergency room management of critically injured patients: a multi-slice CT-oriented care algorithm, Injury 38 (5) (2018) 552–558.

[6] A.A. Weaver, S.L. Schoell, J.D. Stitzel, Morphometric analysis of variation in the ribs with age and sex, J. Anat. 225 (August 2) (2014) 246–261.

[7] H. Ringl, M. Lazar, M. Töpker, R. Woitek, H. Prosch, U. Asenbaum, et al., The ribs unfolded - a CT visualization algorithm for fast detection of rib fractures: effect on sensitivity and specificity in trauma patients, Eur. Radiol. 25 (July 7) (2015) 1865–1874.

[8] G. Bier, C. Schabel, A. Othman, M.N. Bongers, J. Schmehl, H. Ditt, et al., Enhanced reading time efficiency by use of automatically unfolded CT rib reformations in acute trauma, Eur. J. Radiol. 84 (11) (2018) 2173–2180.

[9] P. Dankerl, H. Seuss, S. Ellmann, A. Cavallaro, M. Uder, M. Hammon, Evaluation of rib fractures on a single-in-plane image reformation of the rib cage in CT examinations, Acad. Radiol. 24 (2) (2018) 153–159.

[10] C. Tobon-Gomez, T. Stroud, J. Cameron, D. Elcock, A. Murray, D. Wyeth, et al., OpenRib clinical application, Computational Methods and Clinical Application in Musculoskeletal Imaging, MICCAI-MSKI2017, 2017, pp. 35–45.

[11] S. Khung, P. Masset, A. Duhamel, J.-B. Faivre, T. Flohr, J. Remy, et al., Automated 3D rendering of ribs in 110 polytrauma patients: strengths and limitations, Acad. Radiol. 24 (2) (2018) 146–152.

[12] P.A. Glemser, M. Pfleiderer, A. Heger, J. Tremper, A. Krauskopf, H.-P. Schlemmer, et al., New bone post-processing tools in forensic imaging: a multi-reader feasibility study to evaluate detection time and diagnostic accuracy in rib fracture assessment, Int. J. Legal Med. 131 (March 2) (2017) 489–496.

[13] G. Homann, D.F. Mustafa, H. Ditt, W. Spengler, H.-G. Kopp, K. Nikolaou, et al., Improved detection of bone metastases from lung cancer in the thoracic cage using 5- and 1-mm axial images versus a New CT software generating rib unfolding images, Acad. Radiol. 22 (4) (2018) 505–512.

[14] G. Homann, K. Weisel, D.F. Mustafa, H. Ditt, K. Nikolaou, M. Horger, Improvement of diagnostic confidence for detection of multiple myeloma involvement of the ribs by a new CT software generating rib unfolded images: comparison with 5- and 1-mm axial images, Skeletal Radiol. 44 (July 7) (2015) 971–979.